Proceedings of GREAT Day

Volume 2011 Article 4

2012

Stability Analysis of FitzHugh–Nagumo with Smooth Periodic Forcing

Tyler Massaro
SUNY Geneseo

Stability Analysis of FitzHugh – Nagumo with Smooth Periodic Forcing

Tyler Massaro

1 Background

As Izhikevich so aptly put it,

"If somebody were to put a gun to the head of the author of this book and ask him to name the single most important concept in brain science, he would say it is the concept of a *neuron*[16]."

By no means are the concepts forwarded in his book restricted to brain science. Indeed, one may use the same techniques when studying most any physiological system of the human body in which neurons play an active role. Certainly this is the case for studying cardiac dynamics.

On a larger scale, neurons form an incredibly complex network that branches to innervate the entire body of an organism; it is estimated that a typical neuron communicates directly with over 10,000 over neurons [16]. This communication between neurons takes the form of the delivery and subsequent reception of a traveling electric wave, called an *action potential*[1]. These action potentials become the subject of Hodgkin and Huxley's groundbreaking research.

At any given time, the neuron possesses a certain voltage difference across its membrane, known as its potential. To keep the membrane potential regulated, the neuron is constantly adjusting the flow of ions into and out of the cell. The movement of any ion across the membrane is detectable as an electric current. Hence, it follows, that any accumulation of ions on one side of the membrane or the other will result in a change in the membrane potential. When the membrane potential is 0, there is a balance of charges inside and outside of the membrane.

Before we begin looking at Hodgkin and Huxley's model, we must first understand *how* the membrane adjusts the flow of ions into and out of the cell. Within the cell, there is a predominance of potassium, K^+, ions. To keep K^+ ions inside of the cell, there are pumps located on the membrane that use energy to actively transport K^+ in but not out. Leaving the cell is actually a much easier task for K^+: there are *leak channels* that "randomly flicker between open and closed states no matter what conditions are inside or outside the cell...when they are open, they allow K^+ to move freely[1]."

Since the concentration of K^+ ions is so much higher inside the cell than outside, there is a tendency for K^+ to flow out of these leak channels along its concentration gradient. When this happens, there is a negative charge left behind by the K^+ ions immediately leaving the cell. This build-up of negative charge is actually enough to, in a sense, catch the K^+ ions in the act of leaving and momentarily halt the flow of charge across the membrane. At this precise moment, "the electrochemical gradient of K^+ is zero, even though there is still a much higher concentration of K^+ inside of the cell than out[1]." For any cell, the *resting membrane potential* is achieved whenever the total flow of ions across the cell membrane is balanced by the charge existing inside of the cell. We may use an adapted version of the *Nernst Equation* to determine the resting membrane potential with respect to a particular ion[1]:

$$V = 62\log_{10} Co/Ci,$$

where V is the membrane potential (in mV), C_o is the ion concentration outside of the cell, and C_i is the ion concentration inside of the cell.

Before we continue, it is important to revisit the concept of action potentials. Neurons communicate with each other through the use of electric signals which alter the membrane potential on the recipient neuron. To continue propogating this message, the change in membrane potential must travel the length of the entire cell to the next recipient. Across short distances, this is not a problem. However, longer distances prove to be a bit more of a challenge. To compensate for any amplification that may need to take place, the input of an amount of electrical stimulation beyond a certain threshold yields our aforementioned action potential. These action potentials can carry messages at speeds of up to 100 meters per second[1].

Physiologically speaking, there are some key events taking place whenever an action potential is discharged. Once the cell receives a sufficient electrical stimulus, the membrane is rapidly depolarized; that is to say, the membrane potential becomes less negative. The membrane depolarization causes voltage-gated Na^+ channels to open. (At this point, we have not yet discussed the

role of sodium in the cell. The important thing to understand is that the concentration of sodium is higher outside of the cell than on the inside.) When these Na^+ channels open up, they allow sodium ions to travel down their concentration gradient into the cell. This in turn causes more depolarization, which causes more channels to open. The end result, occurring in less than 1 millisecond, is a shift in membrane potential from its typical resting value of about -60mV to somewhere around +40mV[1]. The value of +40mV actually represents the resting potential for sodium, and so at this point no more sodium ions are entering the cell.

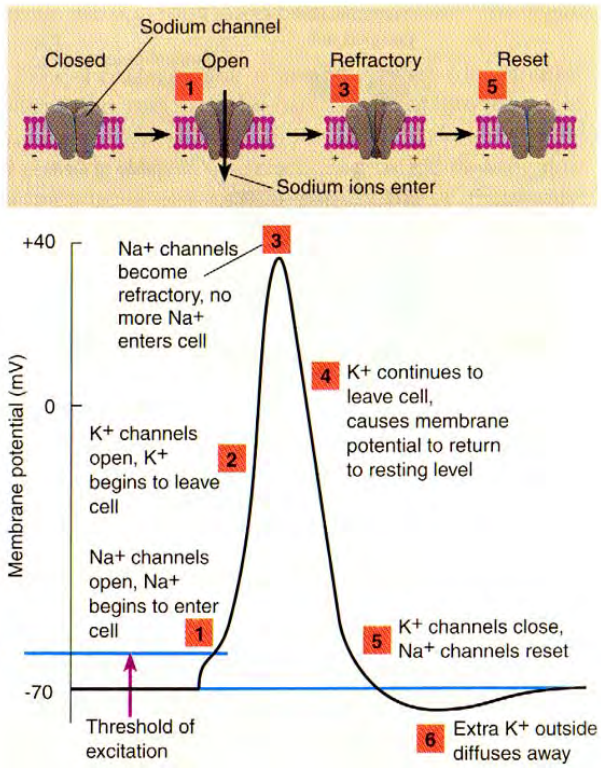

Figure 1 - Diagram of Action Potential
http://internal.psychology.illinois.edu/~etaylor4/action_potential.jpg

Before the cell is ready to respond to another signal, it must first return to its resting membrane potential. This accomplished in a couple of different ways. First, once all of the sodium channels have opened, they switch to an inactive conformation which prevents them from opening back up (imagine putting up a wall in front of an open door). Since the membrane is still depolarized at this point, the gates will stay open. This inactive conformation will persist as long as the membrane is sufficiently depolarized. Once the membrane potential goes back down, the sodium channels switch from inactive to closed [1].

At the same time that all of this occurring, there are also potassium channels that have been opened due to the membrane depolarization. There is a time lag which prevents the potassium gates from responding as quickly as those for sodium. However, as soon as these changes are opened , the K^+ ions are able to travel down their concentration gradient out of the cell, carrying positive charges out with them. The result is a sudden *re*-polarization of the cell. This causes it to return to its resting membrane potential, and we start the process all over again [1].

As a special note of interest, cardiac cells are slightly different from nerve cells in that there are actually two repolarization steps taking place once the influx of sodium has sufficiently depolarized the cell: *fast* repolarization from the exit of K^+ ions, and *slow* repolarization that takes place due to an increase in Ca^{2+} conductance [26]. For now, we will continue dealing solely with Na^+ and K^+.

At this point, it is time to take a look at the models these physiological processes inspired. Arguably the most important of these was created by Alan Lloyd Hodgkin and Andrew Huxley, two men who forever changed the landscape of mathematical biology, when in 1952, they modeled the neuronal dynamics of the squid giant axon. Below are listed the complete set of space-clamped Hodgkin-Huxley equations [14, 16]:

$$C\dot{V} = I - \overbrace{\bar{g}_K n^4 (V - E_K)}^{I_K} - \overbrace{\bar{g}_{Na} m^3 h (V - E_{Na})}^{I_{Na}} - \overbrace{g_L (V - E_L)}^{I_L}$$
$$\dot{n} = \alpha_n(V)(1-n) - \beta_n(V)\, n$$
$$\dot{m} = \alpha_m(V)(1-m) - \beta_m(V)\, m$$
$$\dot{h} = \alpha_h(V)(1-h) - \beta_h(V),$$

where

$$\alpha_n(V) = 0.01\frac{10-V}{\exp\left(\frac{10-V}{10}\right)-1},$$
$$\beta_n(V) = 0.125\exp\left(\frac{-V}{80}\right),$$
$$\alpha_m(V) = 0.1\frac{25-V}{\exp\left(\frac{25-V}{10}\right)-1},$$
$$\beta_m(V) = 4\exp\left(\frac{-V}{18}\right),$$
$$\alpha_h(V) = 0.07\exp\left(\frac{-V}{20}\right),$$
$$\beta_h = \frac{1}{\exp\left(\frac{30-V}{10}\right)+1}.$$

The *E* values represent shifted Nernst equilibrium potentials, *C* is the capacitance, and the *g*,*g* values represent maximal conductances. Our state variables are as follows: *V* is the membrane potential, and *m*, *n*, *h* are the activation variable for

the voltage-gated transient sodium current (there are three), the voltage-gated persistent potassium current (there are four), and the inactivation gate (there is only one), respectively. Each of the activation variables represents the empirically determined probability that a particular channel will be open based upon the current membrane potential.

To provide some background, let us consider two equations from physics. Our first is the standard version of *Ohm's Law*[27]:

$$V = IR,$$

where V is the total voltage of a circuit, I is the total current, and R is the total resistance. Our second equation is *Ohm's Law for Capacitors* [27]:

$$CV = I,$$

where C is the total capacitance, V is the change in voltage, and I is the instantaneous current passing through the capacitor.

Returning to the first line of the H-H equations, we see that this is simply an implementation of Ohm's Law for Capacitors, with the right-hand side showing a total summation of currents for each particular channel, plus the injected current, I. The terms of each of the currents may look somewhat unfamiliar, since they include the product of the conductance, a voltage, and a value representing the percentage of those particular channels that are open. Recall that conductance is simply the inverse of resistance, and it is apparent now that each of these terms may be derived from *Ohm's Law*. In general, we have the following equation, given particular membrane conductances (g_i's) and reverse potentials (E_i's) [16]:

$$C\dot{V} = I - \sum_i g_i (V - E_i).$$

Taking a look at the next three lines, we see the equations for the activation of variables. The α and β terms represent the different Boltzmann and Gaussian functions, which together describe the steady-state activation curve for each particular gating variable [16]. In other words, *m*, *n*, and *h* represent, respectively, the voltage-dependent probability that the sodium, potassium or inactivation gate is open.

Shortly after Hodgkin and Huxley published their model, biophysicist Richard FitzHugh began an in-depth analysis of their work. He discovered that, while their model accurately captures the excitable behavior exhibited by neurons, it is difficult to fully understand *why* the math is in fact correct. This is due not to any oversight on the part of Hodgkin and Huxley, but rather because their model exists in four (4) dimensions. To alleviate this problem, FitzHugh proposed his own two-dimensional differential equation model. It combines a model from Bonhoeffer explaining the "behavior of passivated iron wires," as well as a generalized version of the van der Pol relaxation oscillator [14]. His equations, which he originally titled the Bonhoeffer-van der Pol (BVDP) oscillator, are shown below [14, 26]:

In his model, for which Jin-Ichi Nagumo constructed the equivalent circuit the following year in 1962, x "mimics the membrane voltage," while y represents a recovery variable, or "activation of the outward current [16]." Both a

$$\begin{cases} \dot{x} = c\left(y + x - x^3/3 + z\right), \\ \dot{y} = -\left(x - a + by\right)/c, \end{cases}$$

$$1 - 2b/3 < a < 1, \quad 0 < b < 1, \quad b < c^2.$$

and b are constants he supplied (in his 1961 paper, FitzHugh fixes $a = 0.7$ and $b = 0.8$). The third constant, c, is left over from the derivation of the BVDP oscillator (he fixes $c = 3$). The last variable, z, represents the injected current. It is important to note that in the case of $a = b = z = 0$, the model becomes the original van de Pol oscillator [14].

Many different versions of this model exist [16, 17, 26], all of them differing by some kind of transform of variables. We will consider the model used by Kostova et al. in their paper, which presents the FitzHugh-Nagumo model without diffusion:

$$\begin{cases} \dfrac{du}{dt} = \varepsilon g(u) - w + I, \\ \dfrac{dw}{dt} = u - aw, \end{cases}$$

where $g(u) = u(u - \lambda)(1 - u)$, $0 < \lambda < 1$ and $a, \varepsilon > 0$ [17]. Here, the state variable u is the voltage, w is the recovery variable, and I is the injected current.

2 Stability Analysis via a Linear Approximation

2.1 Examining the Nullclines

When studying dynamical systems, it is important to be familiar with the concept of nullclines. In a broader sense, a nullcline is simply an isocline, or a curve along which the value of a derivative is constant. In particular, the nullcline is the curve along which the value of the derivative is zero. Taking another look at FH-N (1.1), we see that there are two potential nullclines, one where the derivative of u will be zero, and the other where the derivative of w will be zero:

$$\begin{cases} \dfrac{du}{dt} = \varepsilon g(u) - w + I = 0, \\ \dfrac{dw}{dt} = u - aw = 0. \end{cases}$$

One of these nullclines is cubic, and the other is linear. Consider an intersection of those two graphs. At that particular point, we know that

$$\frac{du}{dt} = \frac{dw}{dt} = 0.$$

Hence, at this point, neither of our equations is changing. This point where our nullclines intersect is called an equilibrium, or fixed point. Since our nullclines are cubic and a line, geometrically we see that there could be as many as three possible intersections, and no fewer than one. Let us consider the case where $I = 0$. Our system becomes:

$$\begin{cases} \dfrac{du}{dt} = \varepsilon g(u) - w = 0, \\ \dfrac{dw}{dt} = u - aw = 0. \end{cases}$$

Evaluating the system at the origin, where $u = w = 0$, we can see that this is always an equilibrium when $I = 0$.

2.2 Linearizing FitzHugh - Nagumo

Unless otherwise state, we will assume $I = 0$ for the next few sections. Similarly, (u_e, w_e) will always refer to an equilibrium of FH-N (not necessarily the origin). Let us define the functions f_1 and f_2 as the following:

$$f_1 := \varepsilon g(u) - w + I,$$
$$f_2 := u - aw.$$

Finally, we also set $b_1 = g^1(u_e)$, a notation we get from Kostova et al. [17].

2.2.1 Creating a Jacobian

We may linearize FH-N by constructing a Jacobian Matrix as follows:

$$J(u,w) := \begin{bmatrix} \dfrac{\partial f_1}{\partial u} & \dfrac{\partial f_1}{\partial w} \\ \dfrac{\partial f_2}{\partial u} & \dfrac{\partial f_2}{\partial w} \end{bmatrix}.$$

$$J(u_e,w_e) := \begin{bmatrix} \varepsilon b_1 & -1 \\ 1 & -a \end{bmatrix}.$$

We see that for any equilibrium, $J(u_e, w_e)$ has the same form, since we have the substitution in place for b_1. Thus, we may generalize the eigenvalues of the above Jacobian to be the eigenvalues of any equilibrium. Solving the characteristic polynomial for our Jacobian, we get the following eigenvalues:

$$\mu_{1,2} = \frac{1}{2}(\varepsilon b_1 - a) \pm \frac{1}{2}\sqrt{(a - \varepsilon b_1)^2 + 4(a\varepsilon b_1 - 1)}.$$

As long as it is never the case that $\mathrm{Re}(\mu_1) = \mathrm{Re}(\mu_2) = 0$, the eigenvalues will always have a real part, and then our equilibrium is hyperbolic (see definition below). By the *Hartman - Grobman Theorem*, we know that we may use the Jacobian to analyze the stability of any fixed point of FH-N.

Hyperbolic Fixed Points (2-D). If $\mathrm{Re}(\mu) \neq 0$ for both eigenvalues, the fixed point is *hyperbpolic* [29].

The Hartman-Grobman Theorem. The local phase portrait near a hyperbolic fixed point is "topologically equivalent" to the phase portrait of the linearization; in particular, the stability type of the fixed point is faithfully captured by the linearization. Here topologically equivalent means that there is a homeomorphism that maps one local phase portrait onto the other, such that trajectories map onto trajectories and the sense of time is preserved [29].

2.2.2 *Trace, Determinant, and Eigenvalues*

From Poole [24], we find two results which tie together the trace, J, and determinant,), of a matrix with its eigenvalues. For any *n* x *n* matrix, *A*, with a complete set of eigenvalues, (μ_1, μ_2,...μ_n), we know:

$$\Delta_A = \mu_1\mu_2\ldots\mu_n, \text{ and}$$
$$\tau_A = \mu_1 + \mu_2 + \ldots + \mu_n.$$

For our Jacobian evaluated at an equilibrium, we have:

$$\Delta_J = 1 - \varepsilon b_1 a,$$
$$\tau_J = \varepsilon b_1 - a.$$

Using the table in theorem 12.2.1 (see below, Figure 2) from Nagle [23], we may find the different types of fixed points for each given pair of eigenvalues. We now explore the different stability cases for a given set of real eigenvalues.

Figure 2 – Stability of Linear Systems [23]

Theorem 1. Assume the origin (0, 0) is an isolated critical point for the linear system

$$x'(t) = ax + by,$$
$$y'(t) = cx + dy,$$

where a, b, c, and d are real and $ad - bc \neq 0$. Let r_1 and r_2 be the roots of the characteristic equation

$$r^2 - (a + d)r + (ad - bc) = 0.$$

The stability of the origin and the classification of the origin as a critical point depends on the roots r_1 and r_2 as follows:

Roots	Type of Critical Point	Stability
distinct, positive	improper node	unstable
distinct, negative	improper node	asymptotically stable
opposite signs	saddle point	unstable
equal, positive	proper or improper node	unstable
equal, negative	proper or improper node	asymptotically stable
complex-valued:		
positive real part	spiral point	unstable
negative real part	spiral point	asymptotically stable
pure imaginary	center	stable

Case 1. Let $\varepsilon a b_1 < 1$. Then $\Delta_J > 0$. Evaluating the trace, we see that for $\varepsilon b_1 > a$, we get $\tau_J > 0$, which therefore means that we have a dominate positive eigenvalue. Since $\Delta_J > 0$, we know that both of our eigenvalues must then be positive. This gives us an unstable source. For $\varepsilon b_1 < a$, we get $\tau_J < 0$. This time however, since $\Delta_J > 0$, both of our eigenvalues are negative, and so the system is a stable sink.

Case 2. Let $\varepsilon a b_1 > 1$. Then $\Delta_J < 0$. Hence, our eigenvalues are different signs. In this case, the equilibrium is an unstable saddle.

2.3 *Bifurcation Analysis*

An important area to study in the field of dynamics is *bifurcation theory*. A bifurcation occurs whenever a certain parameter in a system of equations is changed in a way that results in the creation or destruction of a fixed point. Although there are many different classifications of bifurcations, we will focus only on one.

2.3.1 *Hopf Bifurcation*

Consider the complex plane. In a 2-D system, such as FH-N, a stable equilibrium will have eigenvalues that lie in the left half of the plane, that is, the Re(μ) < 0 half of the plane. Since these eigenvalues in general are the solutions to a particular quadratic equation, we need them both to be either real or negative, or complex conjugates in the same Re(μ) < 0 part of the plane. Given a stable equilibrium, we may de-stabilize it by moving one or both of the eigenvalues to the Re(μ) > 0 part of the complex plane. Once an equilibrium has been de-stabilized in this manner, a *Hopf bifurcation* has occurred [29].

2.3.2 *Proposition 3.1 (From Kostova)*

As the eigenvalues μ_1, μ_2 *of any equilibrium* (μ_1, μ_2) *are of the form*

$$\mu_{1,2} = \frac{1}{2}R(\varepsilon, a, b_1) \pm \frac{1}{2}\sqrt{R^2 + 4Q}$$

where $Q(\varepsilon, a, b_1) \equiv \varepsilon, a, b_1 - 1$ *and* $R \equiv \varepsilon b_1 -$ *a Hopf bifurcation occurs in cases when* $R = 0$ *and* $Q < 0$ [17].

Proof. Recall from earlier that we defined the Jacobian for FH-N as follows:

$$J(u, w) = \begin{bmatrix} \varepsilon g'(u) & -1 \\ 1 & -a \end{bmatrix}.$$

Now we solve for the eigenvalues of this matrix evaluated at an equilibrium. For equation 2.1 we know our eigenvalues have the following form:

$$\mu_{1,2} = \frac{1}{2}(\varepsilon b_1 - a) \pm \frac{1}{2}\sqrt{(a - \varepsilon b_1)^2 - 4(-a\varepsilon b_1 + 1)}.$$

Substituting in now for R and Q, we clearly have $\mu_{1,2} = \frac{1}{2}R \pm \frac{1}{2}\sqrt{R^2 + 4Q}$.

If we allow $Q < 0$ and $R = 0$, our eigenvalues become:

$$\mu_{1,2} = \pm\frac{1}{2}\sqrt{4Q} = \pm i\sqrt{Q}.$$

Both of these eigenvalues are along the imaginary axis. This is the exact point at which Hopf bifurcation occurs.

3 Stability Analysis via Lyapunov's Second Method

At the end of nineteenth century, Russian mathematician Aleksandr Lyapunov developed an entirely new approach to analyzing the stability of nonlinear systems. His technique, now referred to as the direct method, yields more insights about equilibrium stability than the comparable linear approach. Specifically, in addition to standard classification of fixed points, one may also assess regions of asymptotic stability. However, more thorough results come at the cost of requiring the use of special auxiliary functions [6]. The ability to create these functions has been described as more of an art than an actual science, with one author going so far as to suggest that "[d]ivine intervention is usually required... [29]." In this next section, we analyze the Lyapunov functional published by Kostova et al. in their paper [17].

3.1 Defining Positive and Negative Definite

Primary among these auxiliary functions, and described in terms of conservation laws, are the total energy of a system, V , and its derivative, which Brauer and Nohel refer to as V †. Keeping these in mind, it is important to become familiar with the definitions described below for a function which is positive or negative definite in a region centered about the origin. Later on, we will consider regions of positive or negative definiteness centered about an equilibrium of FH-N (1.1), by shifting this equilibrium to the origin.

Positive Definite. The scalar function V $\left(\underset{y}{\rightarrow}\right)$ is said to be *positive definite* on the set Ω if and only if V $\left(\underset{0}{\rightarrow}\right)$ = 0 and V $\left(\underset{y}{\rightarrow}\right)$ > 0 for ≠ 0 and $\underset{y}{\rightarrow}$ in Ω [6].

Negative Definite. The scalar function V $\left(\underset{y}{\rightarrow}\right)$is *negative definite* on the set Ω if and only if –d V $\left(\underset{y}{\rightarrow}\right)$ is positive definite on Ω [6].

Derivative of V. The derivative of V with respect to the system $\underset{y^1}{\rightarrow}$= $f\left(\underset{y}{\rightarrow}\right)$ is the scalar product V*$\left(\underset{y}{\rightarrow}\right)$ = grad V $\left(\underset{y}{\rightarrow}\right)$ • $f\left(\underset{y}{\rightarrow}\right)$

$$= \frac{\partial V}{\partial y_1}(\vec{y}) f_1(\vec{y}) + \frac{\partial V}{\partial y_2}(\vec{y}) f_2(\vec{y}) + \ldots + \frac{\partial V}{\partial y_n}(\vec{y}) f_n(\vec{y})$$ [6].

In terms of the FitzHugh-Nagumo model, Kostova et al. offer the following for V (u, w)

$$V(u,w) = \frac{1}{2}[u - u_e - a(w - w_e)]^2 + G(w - w_e),$$

where $G(x) = \frac{1}{4}\varepsilon a x^2\left[a^2x^2 - \frac{4}{3}axb_2 - 2\left(b_1 - \frac{1}{a\varepsilon}\right)\right]$. By definition, we may also find $V^*(u,w)$, $\dot{V}(u,w)$.

Before we continue, the direct method requires that our function, V (u, w), be positive definite. Suppose we have some region, Ω, of the u, w-plane, which encloses an equilibrium, (u_e, w_e). Evaluating V (u_e, w_e), we get:

$$V(u_e, w_e) = \frac{1}{2}[u_e - u_e - a(w_e - w_e)]^2 + G(w_e - w_e)$$

$$= 0.$$

This however is not enough to guarantee that V will be positive definite. We must now verify that V (u, w), > 0∀ $(u,w)\epsilon\Omega(u_e, w_e)$. To do this, we will need some notation from Kostova:

$$T = (1 - \varepsilon b_1 a) - \frac{2\varepsilon a b_2^2}{9}$$

and

$$S = \frac{b_2^2}{3} + b_1 - \frac{a}{\varepsilon}$$

where $b_{1=\mathbb{g}'(u_e)}$ and $b_2 = \frac{\mathbb{g}''(u_e)}{2}$ (refer to the line immediately following equation 1.1 for a definition of g(u)).

Let line L be defined by $L = \{(u,w)|u = u_e + aw - we.$

3.1.1 Proposition 2.2a (from Kostova)

V (u,w)> 0 for all $(u,w) \neq (u_e, w_e)$*if and only if* $T > 0$. *If* $T \leq 0$, *then* $V \leq 0$ *is a bounded set B, which is symmetric about the line L* [17].

Proof. Consider a Taylor series expansion of g(u) at the equilibrium, taking note that the terms of order 4 or greater vanish:

$$g(u) = g(u_e) + g'(u_e)(u - u_e) + \frac{1}{2}g''(u_e)(u - u_e)^2 + \frac{1}{6}g^{(3)}(u_e)(u - u_e)^3.$$

We see that $g^{(3)}(u) \equiv -6\ \forall u \in \mathbb{R}$. Making this and two other substitutions for b_1 and b_2, we get:

$$g(u) = g(u_e) + b_1(u - u_e) + b_2(u - u_e)^2 - (u - u_e)^3.$$

Before we continue, we first go back to FH-N. By definition, we know that $\frac{du}{dt} = \frac{dw}{dt} = 0$ at the equilibrium. Evaluating the system at the equilibrium, we get the following two results:

$$\begin{cases} \varepsilon g(u_e) = w_e \\ u_e = a w_e. \end{cases}$$

At this point, recall how the definitions for positive and negative definiteness provided at the beginning of the section require V(u,w) to be 0 at the origin of

the system. Thus far, we have only been considering regions that surround some general equilibrium. However, from section 2.1, we know that the origin will always be an equilibrium whenever I = 0. By introducing these transformations from Kostova, we may easily translate all of our functions to be situated around the origin:

$$v = u - u_e, \quad s = w - w_e, \quad v - as = y, \quad s = x,$$

The original FH-N system (1.1) becomes:

$$\begin{cases} \frac{dx}{dt} = y \\ \frac{dy}{dt} = -yf(x,y) - g_1(x), \end{cases} \tag{3.1}$$

where

$$f(x,y) = \varepsilon\left(y^2 + (3ax - b_2)y + (3a^2x^2 - 2b_2ax - b_1)\right) + a,$$
$$g_1(x) = -\varepsilon\left(b_1ax + b_2a^2x^2 - a^3x^3\right) + x.$$

The line L is now described by the equation y = 0. Note that V and G have also changed:

$$V(x,y) = \frac{1}{2}y^2 + G(x),$$

$$G(x) = \int_0^x g_1(\xi)\, d\xi.$$

At this point, there are well-documented methods for determining Lyapunov functionals in a system of the form seen above in equation 3.1 [4].

Consider V (x, y). We know that $\frac{1}{2}y^2 \geq 0 \; \forall y \in \mathbb{R}$. To better understand V (x, y) we must focus our attention on G(x).
Recall that

$$G(x) = \frac{1}{4}\varepsilon a x^2\left[a^2x^2 - \frac{4}{3}axb_2 - 2\left(b_1 - \frac{1}{a\varepsilon}\right)\right].$$

Already we know that $\frac{1}{4}\varepsilon a x^2\left[a^2x^2 - \frac{4}{3}axb_2 - 2\left(b_1 - \frac{1}{a\varepsilon}\right)\right]$. Now, we must consider the other term. By completing the square, we see that

$$a^2x^2 - \frac{4}{3}axb_2 - 2\left(b_1 - \frac{1}{a\varepsilon}\right)$$

becomes

$$\left(x - \frac{2}{3a}b_2\right)^2 - \frac{2}{a^2}\left(b_1 - \frac{1}{a\varepsilon}\right) - \frac{4}{9a^2}b_2^2.$$

After some algebra, we introduce the constant T as described at the beginning of our proof, giving us:

$$V(x,y) = \frac{1}{2}y^2 + \frac{1}{4}\varepsilon a x^2\left[\left(x - \frac{2}{3a}b_2\right)^2 + \frac{2}{a^3\varepsilon}T\right].$$

Case 1. Let $T \geq 0$. Then, $V(x,y) > 0 \; \forall (x,y) \neq (0,0)$.

Case 2. Let $T < 0$. Then the level curves of V are closed curves, symmetric about the x-axis. These level curves enclose the region which we have previously described as $\mathcal{B}$. Shown below is the zero level curve of $V(x,y)$.

Figure 3 – $V(x,y) = 0; I = 0, a = 1.2, \lambda = 0.1, \varepsilon = 14, (u_e, w_e) = (0,0)$.

Up to this point, we have determined regions in which V is positive or negative definite. Before we may begin assessing the stability of FH-N, we must find similar regions of positive and negative definiteness for V.

3.1.2 *Proposition 2.2b (from Kostova)*

On L the derivative $\dot{V} = \frac{\partial V}{\partial u}u + \frac{\partial V}{\partial w}w = 0$. *Additionally,* $\dot{V} < 0$ *if* $S < 0$ *and* $(u,w) \notin L$. *If* $S \geq 0$ *there exists an ellipse* ∂E, *surrounding a region* E *such that : i)* $\dot{V} < 0$ *if* (u,w) *belongs to the complement of* $\partial E \cup E \cup L$; *ii)* $\dot{V} > 0$ *if* $(u,w) \in {}^{E}/_{L}$.[17].

Proof. Let us first make a change of variables to V. by definition, we have that:

$$\dot{V}(x,y) \equiv \frac{\partial V}{\partial x}\dot{x} + \frac{\partial V}{\partial y}\dot{y}.$$

Borrowing from calculations performed during the proof in Section 3.1.1, we get:

$$\dot{V}(x,y) \equiv G'(x)\,y + y\left(-yf(x,y) - g_1(x)\right)$$
$$\equiv \left[\frac{d}{dx}\int_0^x g_1(\xi)\, d\xi\right] y + y\left(-yf(x,y) - g_1(x)\right)$$
$$\equiv -y^2 f(x,y).$$

Recall also that the line L has the equation y = 0. It is then clear that V(x, y) = 0 on L, which includes the origin. To make further insights about V(x, y) however, we must consider f (x, y). From before, we have:

$$f(x,y) = \varepsilon\left(y^2 + (3ax - b_2)y + (3a^2x^2 - 2b_2ax - b_1)\right) + a.$$

Rearranging terms, we get:

$$\frac{1}{\varepsilon}f(x,y) = \left(y^2 + (3ax - b_2)y + \left(3a^2x^2 - 2b_2ax - b_1 + \frac{a}{\varepsilon}\right)\right).$$

Completing the square for a quadratic with respect to y, we get

$$\frac{1}{\varepsilon}f(x,y)=\left(y+\left(\frac{3ax-b_2}{2}\right)\right)^2+\left(3a^2x^2-2b_2ax-b_1+\frac{a}{\varepsilon}\right)$$
$$-\frac{1}{4}\left(9a^2x^2-6b_2ax+b_2^2\right).$$

Once again, we complete the square, this time using constant terms with respect to *y*:

$$\frac{1}{\varepsilon}f(x,y)=\left(y+\left(\frac{3ax-b_2}{2}\right)\right)^2+\left(3a^2-\frac{9}{4}a^2\right)x^2+\left(-2b_2a+\frac{6}{4}b_2a\right)x$$
$$+\left(-b_1+\frac{a}{\varepsilon}-\frac{1}{4}b_2^2\right)$$
$$\vdots$$
$$=\left(y+\left(\frac{3ax-b_2}{2}\right)\right)^2+\left(x-\frac{b_2}{3a}\right)^2-\frac{4}{3a^2}\left(\frac{b_2^2}{3}+b_1-\frac{a}{\varepsilon}\right).$$

Now we substitute back in for *S*, seeing that our expression becomes

$$\frac{1}{\varepsilon}f(x,y)=\left(y+\left(\frac{3ax-b_2}{2}\right)\right)^2+\left(x+\frac{b_2}{3a}\right)^2-\frac{4}{3a^2}S.$$

In terms of $\dot{V}$, we now have:

$$\dot{V}(x,y)=-\varepsilon y^2\left[\left(y+\left(\frac{3ax-b_2}{2}\right)\right)^2+\left(x+\frac{b_2}{3a}\right)^2-\frac{4}{3a^2}S\right]$$

Case 1. Let $S<0$. Then $f(x,y)>0$, and so $\dot{V}(x,y)<0\ \forall\,(x,y)\notin L$.

Case 2. Let $S>0$. Then, for $f(x,y)=0$, we have an ellipse, $\partial\mathcal{E}$, surrounding a region $\mathcal{E}$:

$$f(x,y)=\left(y+\left(\frac{3ax-b_2}{2}\right)\right)^2+\left(x+\frac{b_2}{3a}\right)^2=\frac{4}{3a^2}S.$$

Since $y=0$ along L, we know the following:

$$\dot{V}(x,y)>0\ \forall\,(x,y):(x,y)\in\mathcal{E}\setminus(\partial\mathcal{E}\cup L).$$

3.2 Lyapunov's Theorems for Stability

We have successfully found regions in the *x*, *y*-plane (a transformed version of the u, w-plane) where our function V (x, y) and its derivative V(x, y) are positive or negative definite. The following theorems from Brauer and Nohel provide for us a way to analyze the stability of FH-N in light of the regions we have found.

Theorem 1. If there exists a scalar function $V(\vec{y})$ that is positive definite and for which $V^*(\vec{y})\leq 0$ on some region Ω containing the origin, then the zero solution of $\vec{y}'=f(\vec{y})$ is stable [6].

Theorem 2. If there exists a scalar function $V(\vec{y})$ that is positive definite and for which $V^*(\vec{y})$ is negative definite on some region Ω containing the origin, then the zero solution of $\vec{y}'=f(\vec{y})$ is asymptotically stable [6].

Theorem 3. If there exists a scalar function $V(\vec{y})$, $V(0)=0$, such that $V^*(\vec{y})$ is either positive definite or negative definite on some region Ω containing the origin and if there exists in every neighborhood N of the origin, $N\subset\Omega$, at least one point $a\neq 0$ such that $V(a)$ has the same sign as $V^*(\vec{y})$, then the zero solution of $\vec{y}'=f(\vec{y})$ is unstable [6].

3.2.1 Proposition 2.2c (from Kostova)

If $\varepsilon b_1 a<1$ and $\varepsilon b_1(u_e, w_e)$ which no solution curves of FH-N (3.1) enter. If $\varepsilon b_1 a<1$ and $\varepsilon b_1 < a$, there is a neighborhood of the equilibrium which no solution curve leaves. These neighborhoods can be found explicitly by using level curves of V [17]

Proof. Recall that:

$$V(x,y)=\frac{1}{2}y^2+\frac{1}{4}\varepsilon ax^2\left[\left(x-\frac{2b_2}{3a}\right)^2+\frac{2}{a^3\varepsilon}T\right],$$

where $T=(1-\varepsilon b_1 a)-\frac{2\varepsilon a b_2^2}{9}$.

Case 1. Let $\varepsilon b_1 a<1$. Whenever $1-\varepsilon b_1 a>\frac{2}{9}\varepsilon a b_2^2$, there is some neighborhood of $(u_e, w_e)=(0,0)$ such that $V(x,y)>0$ for all *x* and *y* in that neighborhood. Recall also that before, we defined the set, *B*, such that $V(x,y)\leq 0\ \forall\ (x,y)\in B$. Hence if *B* exists in this case then it does not contain the origin. Consider how $\varepsilon b_1 > a$. Then, we know that *S* (or $\frac{b_2^2}{2}+b_1-\frac{a}{\varepsilon}$), is strictly greater than 0. Hence, $V(x,y)>0\forall\ (x,y)\in E\setminus L$.

Evaluating $f(x,y)$ at the origin, we get:

$$f(0,0)=\varepsilon(-b_1)+a$$
$$=a-\varepsilon b_1.$$

But, we have assumed $\varepsilon b_1 > a$. Then, $f(0,0)<0$. And so, for a neighborhood of the origin, we know that $V(x,y)>0$, except on the line *L*, in which case, $V(x,0)\equiv 0$. And by definition, this region, which contains the origin, must be part of *E*.

For level curves $V(x,y)=c$, $c>0$, we allow that *c* surrounds *B*. At the same time however, we restrict this level curve to be contained entirely within *E*. In this way, there is a region where $V(x,y)>0$ and $V(x,y)>0$. Solutions may exist entirely within *B*, at the origin, or outside of *E* entirely, since *E* is the region where $V(x,y)>0$.

Case 2. Let $\varepsilon b_1 < a$. Then, if $S<0$, either no ellipse *E* exists, or the ellipse does exist, however the origin is no longer inside of it. Consider once again $f(x,y)$ at the origin. We see that $f(0,0)>0$. Hence, $V(x,y)<0$. Recall that our ellipse, *E*, contains the region where $V(x,y)>0$, assuming we restrict $(x,y)\in E\ (E\cap L)$.Our solution curve, $V(x,y)=c$ may exist anywhere so long as it does not intersect *B* or *E*.

Figure 4 – Direction Field for FitzHugh-Nagumo

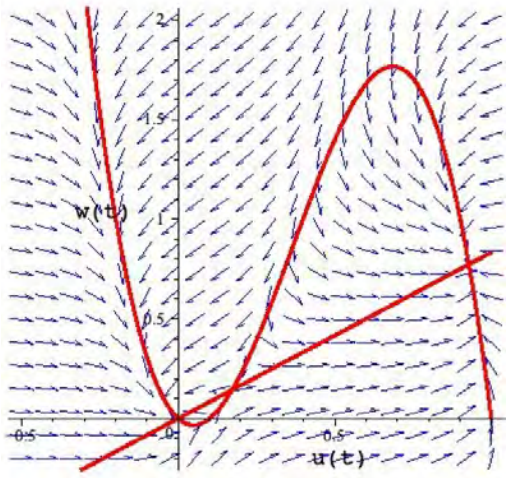

4 Chaos

4.1 Butterflies

We have really only focused on determining the stability of our fixed points, however there are many other interesting questions we can ask of a dynamical system. Two of these questions, which concern sensitivity dependence, we can lump together: how sensitive is our system to the initial conditions that we give it, and how sensitive is our system to a certain parameter which it calls?

The relevance of this first question was explored by meteorologist Edward Lorenz [20]. At the time, he was studying weather forecasting models. He found that by changing his initial input to the system, he could wildly, and quite unexpectedly, change the prediction give by his model. Consider the following question, which was actually the title of a talk given by Lorenz back in 1972 [20]:

Does the Flap of a Butterfly's Wings in Brazil Set Off a Tornado in Texas?

This may at first seem frivolous, but the concept which drove him to ask in the first place digs a little bit deeper. Given some system which you use to make predictions (in essence, any mathematical model), do you expect that using roughly equal initial conditions will give you roughly the same prediction? Surprisingly, and this is what Lorenz discovered, the answer is not always yes.

Granted, this question depends on a lot of things, for instance how far apart your initial conditions are, how far into the future you wish to make predictions, and how different predictions need to be before you are willing to actually deem them "different." However, once we define explicitly what we are asking, we can learn a great deal about our system. When we start thinking about this in mathematical terms, the butterfly effect means that two solutions, initialized ever so slightly apart, will diverge exponentially as time progresses (assuming of course that our system in question possesses this property).

4.2 Modified BVDP with Smooth Periodic Forcing

With regards to the FitzHugh-Nagumo model, asking such a question as to whether it is sensitive to initial conditions is in most cases trivial. If we take a look at the vector field in the phase plane (see above), we see that none of our solutions will run away on some different path, since they are all restricted. You may recall at this point, back in section 3, how we found a region in which V was negative definite.

Figure 5 – Modified BVDP Phase Portrait, $\kappa = 0$.

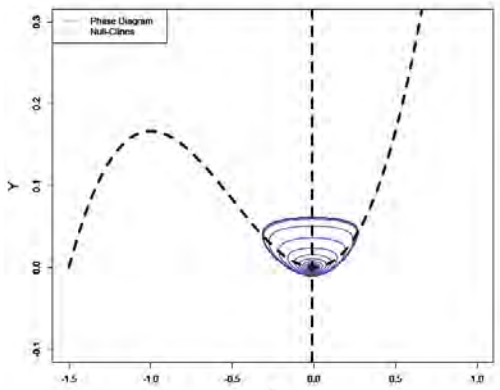

Even more specifically however, we know that each solution starting in a certain neighborhood of the equilibrium will either converge asymptotically to the equilibrium, or it will periodically trace an orbit that is held within the neighborhood. There are no surprises here: as long as you initialize a solution in the neighborhood, you will get asymptotic convergence or an orbit.

But what happens when you start changing the parameters inside of the equations themselves? We will begin to examine this question by considering a modified version of the Bonhoeffer - van der Pol equation [5], which is a distant cousin of the FitzHugh-Nagumo model (remove the forcing function and do a change of variables to get FH-N):

$$\begin{cases} \varepsilon \frac{dx}{dt} &= y - \left(\frac{1}{2}x^2 + \frac{1}{3}x^3\right), \quad 0 < \varepsilon << 1, \\ \frac{dy}{dt} &= -(x+\alpha) + s(t), \quad \alpha \in \mathbb{R}. \end{cases}$$

The authors, Braaksma et al., define $s(t)$ to be a Dirac δ-function calling t modulus some constant, T. While the Dirac function is especially useful for modeling neuronal dynamics, we decided to look at smooth forcing. The function we ultimately ended up choosing is rather simple: We consider a smooth, periodic force, generated by $s(t) = \kappa\cos(t)$.

Consider the modified BVDP oscillator which fixes $\varepsilon = \alpha = 0.01$, and $\kappa = 0$. The phase diagram for a solution starting near the origin is shown in Figure 5. We will take some liberties by assuming that the physiological analog for this solution is similar to that of our original FH-N oscillator. Notice above in Figure 6 how a neuron in the active state could be modeled by a solution, $\Phi(u, w)$, which travels sufficiently far towards the "left" side of the phase space (u decreasing) before travelling up the left knee of the cubic nullcline [14]. Taking a look at the phase portrait for the above conditions (Figure 5), we see that this particular "neuron" never reaches the active state.

Keeping ε and α fixed at their value of 0.01, we now set $\kappa = 0.5$ (Figure 7). In essence, we are delivering a continuously oscillating current of electricity, the magnitude of which does not exceed 0.5. We see now that a solution with the exact same starting conditions now sweeps all the way to the left side of the space before traveling up the left knee. Referencing once again the picture of the phase space for Figure 7, we see that this solution simulates a neuron experiencing an active state (in addition to other states).

Another important aspect of this portrait worth noting is the existence of what appear to be four periodic limit cycles through which our solution travels. Shown in Figure 8 is the *bifurcation diagram* for our bifurcating parameter, κ. We see that as the value of κ changes from 0.1 to 1, solutions exist possessing 2, 3, and 4 distinct limit cycles (we see that it is consistent with the phase portrait for $\kappa = 0.5$). For κ between 0 and 0.1 however, it is unclear what is happening. It appears as though dozens of limit cycles may potential exist. Our system seems o be highly sensitive to the value of κ. The question now becomes whether or not this parameter sensitivity means that chaos is actually present.

Figure 6 – Physiological analogs for solutions to FitzHugh's BVP model [14].

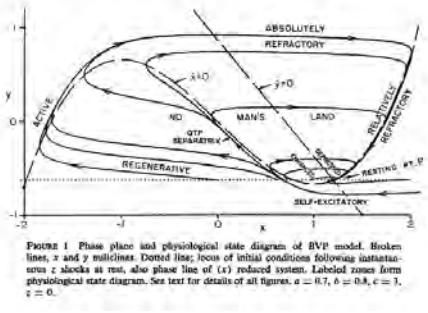

FIGURE 1 Phase plane and physiological state diagram of BVP model. Broken lines, x and y nullclines. Dotted line; locus of initial conditions following instantaneous z shocks at rest, also phase line of (x) reduced system. Labeled zones form physiological state diagram. See text for details of all figures. $a = 0.7$, $b = 0.8$, $\epsilon = 3$, $z = 0$.

Figure 7 – Modified BVDP Phase Portrait, $\kappa = 0.5$.

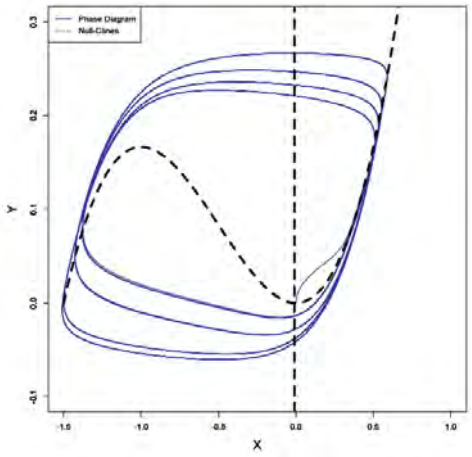

4.3 Lyapunov Exponents

Arguably the most popular way to quantify the existence of chaos is by calculating a *Lyapunov exponent.* An n-dimensional system will have n Lyapunov exponents, each corresponding to the rate of exponential divergence (or convergence) of two nearby solutions in a particular direction of the n-space. A positive value for a Lyapunov exponent indicates exponential divergence; thus, the presence of any one positive Lyapunov exponent means that the system is chaotic [34].

4.3.1 Lyapunov Spectrum Generation

There have been numerous algorithms published outlining different ways for generating what are known as *Lyapunov spectra.* As previously mentioned, an n-dimensional system will have n Lyapunov exponents. Each Lyapunov exponent is defined as the limit of the corresponding Lapunov spectrum calculated using one of these aforementioned algorithms. For our calculations, we consider the following method from Rangarajan which eliminates the need for reorthogonalization and rescaling [25].

Figure 8 – Bifurcation Diagram for κ.

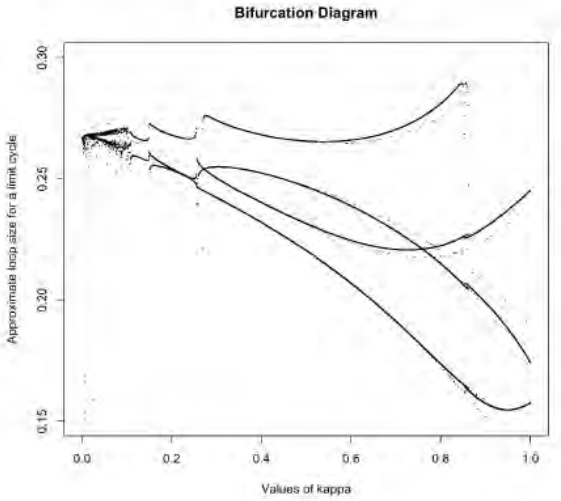

Suppose we have a two dimensional system of nonlinear differential equations, like the one below:

$$\begin{cases} \dfrac{dx_1}{dt} = f_1(x_1, x_2), \\ \dfrac{dx_2}{dt} = f_2(x_1, x_2). \end{cases}$$

We may describe a Jacobian for this system in the same way as we did back in Section 2:

$$J(x_1, x_2) := \begin{bmatrix} \dfrac{\partial f_1}{\partial x_1} & \dfrac{\partial f_1}{\partial x_2} \\ \dfrac{\partial f_2}{\partial x_1} & \dfrac{\partial f_2}{\partial x_2} \end{bmatrix}$$

Given our two dimensional system and its corresponding linearization, Rangarajan introduces three more differential equations to be coupled with the original system. The state variables λ_1 and λ_2 are the Lyapunov exponents, and 2 is a third variable describing angular evolution of the solutions. The heart of the algorithm, equations for setting up the three new variables, is shown below [25]:

$$\begin{cases} \dfrac{d\lambda_1}{dt} = J_{11}\cos^2(\theta) + J_{22}\sin^2(\theta) - \frac{1}{2}(J_{12} + J_{21})\sin(2\theta), \\ \dfrac{d\lambda_2}{dt} = J_{11}\sin^2(\theta) + J_{22}\cos^2(\theta) + \frac{1}{2}(J_{12} + J_{21})\sin(2\theta), \\ \dfrac{d\theta}{dt} = -\frac{1}{2}(J_{11} - J_{22})\sin(2\theta) + J_{12}\sin^2(\theta) - J_{21}\cos^2(\theta). \end{cases}$$

Coupling these three equations with our original system, we get a five dimensional system of differential equations. We now simultaneously solve all of these as we would any other system of differential equations, and the output corresponding to the values of λ_1 and λ_2 over time is the Lyapunov spectrum we seek.

4.3.2 The Lyapunov Spectra

Running the algorithm for our modified BVDP model with 6 = 0.5 will produce the spectrum shown in Figure 9. Recall how we saw four stable limit cycles existing for the solution to this system. Hence, we would not expect either of our Lyapunov exponents to be greater than zero. Upon generating each of the Lyapunov spectra, we see that this is indeed the case. Both of the Lyapunov exponents for this particular system seem to settle down right away at two negative values, a result which is consistent with our expectations. In general, for roughly any system constructed with a 6 value between 0.1 and 1, we can predict, at the very least, that both of our Lyapunov exponents will be less than zero.

Figure 9 – Lyapunov Spectrum for Modified BVDP, κ = 0.5.

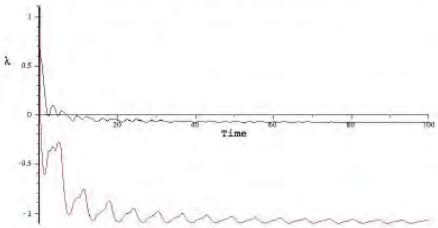

However, the same cannot be said for systems calling a value of 6 between 0 and 0.1. Setting 6 = 0.01, we may generate the following phase portrait (see Figure 10). Notice there are now numerous orbits, none of which are generating an active state, and none of which seem to have been traced more than once. Said another way, this solution, upon first glance at least, appears to be aperiodic. Aperiodicity is our first clue that chaos might be present in the model.

Figure 10 – Modified BVDP Phase Portrait, κ = 0.01.

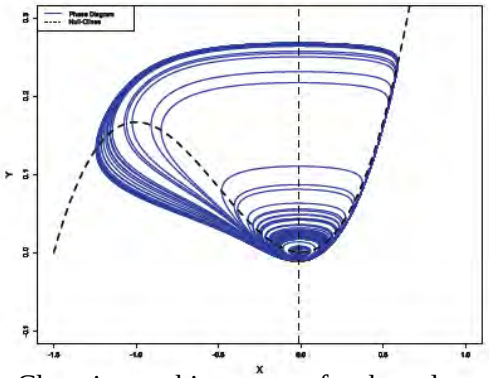

Changing nothing except for the value of 6, we may now generate the Lyapunov spectrum

corresponding to this new system (Figures 11 and 12). We see that one of these lines eventually makes its way underneath the horizontal axis, but the other one hovers enticingly close to the axis. At first glance, it is difficult to tell whether or not it ever actually reaches the horizontal axis and/or goes negative. The figure shown below this current spectrum zooms in on values between $t = 80$ and $t = 100$.

Figure 11 – Lyapunov Spectrum for Modified BVDP, $\kappa = 0.01$.

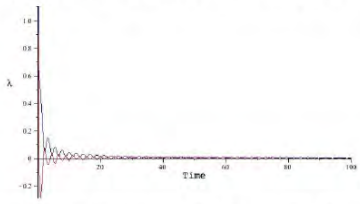

Figure 12 – Lyapunov Spectrum for Modified BVDP, $\kappa = 0.01, 180 \leq t \leq 200$.

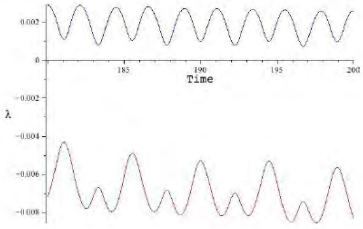

In terms of chaos, it is difficult to judge what is happening. While one of these lines ventures below the horizontal axis, the other is clearly oscillating strictly *above* the axis. We could be remiss to immediately conclude that chaos is in fact present. And we have two reasons for offering this conjecture:

1. The oscillations are being only slightly damped, and

2. There appears to be a decreasing trend to these oscillations, suggesting they may eventually pass beneath the horizontal axis.

The first reason listed above presents issues for us since we need this output to approach some kind of limit. If it continues to behave like it is currently, we cannot say definitively whether it will asymptotically reach a limit or not (recall how the limit of cost*(t)* is undefined as *t* approaches infinity). Should it *not* asymptotically approach a limit, the only real conclusion we could offer is that we need to use a more robust algorithm. The second reason is not so much a problem as it is an observation that this output could be asymptotically approaching a positive, negative, or zero valued limit. For now, all we know is that one of our Lyapunov exponents appears to be negative, and the other is positive as far as our solver can tell us.

5 Discussion

"The healthy heart dances, while the dying organ can merely march [8]"
-Dr. Ary Goldberger, Harvard Medical School

The very nature of cardiac muscle stimulation fosters an environment for the propogation of chaos as we have previously described it. This may at first seem slightly counterintuitive. The word "chaos" itself connotes disorder. Certainly it would not immediately come to mind to describe a process as efficient as cardiac muscle contraction. And yet, what we find physiologically with hear rhythms is that a "...perfectly regular heart rhythm is actually a sign of potentially serious pathologies [10]." In particular, many periodic processes manifest themselves as arrythmia such as ventricular fibrillation or asystole (the absence of any heartbeat whatsoever) [12]. Neither of these particular heart rhythms is conducive for sustaining life: automated external defibrillators (AEDs) were developed to counteract the presence of ventricular fibrillation in a patient; and asystole is the exact opposite of what is conducive for keeping a human alive.

At this point, it would appear as if chaos, at least in humans, is required for survival. Indeed, Harvard researcher Dr. Ary goldberger was so moved by this idea that he made the above comment before a conference of his peers back in 1989. As the next few years unfold, it will be interesting to see what role, if any, chaos plays in assisting engineers with the development of new equipment to alter life-threatening cardiac arrhythmia in patients. The past twenty years especially have seen a tremendous increase in the demand for AEDs in public fora. Unfortunately, commercially available AEDs can only treat ventricular fibrillation and ventricular tachycardia [28].

AEDs operate by applying a burst of electricity along the natural circuitry in the heart. This electrical stimulus causes a massive depolarization event to take place, triggering simultaneous contraction of a vast majority of cardiac cells. The hope is that this sufficiently resets the heart enough for the pacemaker to regain control. In terms of a forcing function, this is almost similar to stimulation via a Dirac *-function. Hence, we find the underlying motivation for our exploration into alternative forcing functions.

If we consider our modified BVDP model to be a sufficient analog to cardiac action potential generation, then the solution in Figure 5 roughly represents a heart experiencing ventricular fibrillation. Application of our forcing function $s(t) = 6\cos(t)$ for amplitudes between 0.1 and 1 seems to positively impact this model by inducing active states. However, it is unknown whether or not this is a realistic or even adequate portrayal of positively intervening on an arrhythmic event.

In light of the quote from Dr. Goldberger, is it possible that we should be discounting periodic solutions? If a healthy heart rhythm is in fact chaotic, would this necessitate the generation of a chaotic solution? Thus far, the closest we have come to the aforementioned chaotic solution is one which nondiscriminantly oscillates along subthreshold or superthreshold orbits, most of which do not even come close to simulating an active event in the cell. In essence, this would imply that the heart is "skipping a beat" each time it fails to generate an action potential. This is no closer to offering a viable heart rhythm, and is actually further off the mark, than our periodic solutions. Unfortunately, our search continues for an induced current that can generate both chaos and muscle contraction.

Another issue needing to be considered is the fact that we cannot, in our modified BVDP model with smooth periodic forcing, remove the forcing lest the neuron quit generating action potentials. Shown below in Figure 13 is the phase portrait for the modified BVDP model with a damped periodic forcing function, $s(t) = \frac{1}{t+1}k\cos(t)$. We see maybe one action potential generated, and then rest are all subthreshold excitations.

At first glance, it would appear as though we have to continuously induce our current. This imposes an entirely impractical, even dangerous, requirement on emergency service providers in the field. However, if our forcing function behaves at all like an AED, this result is not surprising. Once you strip away the forcing function, or in our case, once you evaluate solutions after t has grown sufficiently large, the underlying model describes a v-fib-like event taking place. It would then only make sense that action potentials are no longer generated.

The question now is whether or not our forcing function could effectively take the place of a strong induced electrical spike, similar to that delivered by an AED. And if the answer is no, are there scenarios in which continuous application of our periodic current would be practical? Certainly no such scenario is imaginable for AEDs, however the possibility remains that it could be useful within a highly controlled setting such as inside of an operating room during surgery or built into an implantable pacemaker. Ultimately, this is a question best left to the engineers and surgeons.

Figure 13 – Modified BVDP Phase Portrait, Damped Forcing

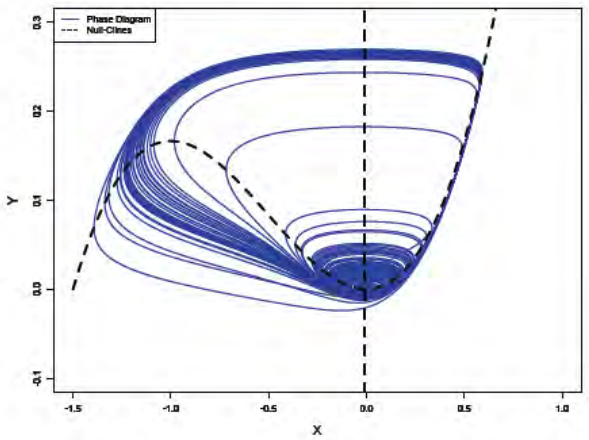

The reason why this is so important is because sudden cardiac arrest (SCA), causes the deaths of more than 250,000 Americans each year [15]. Contrary to popular belief, SCA is first and foremost an electrical problem, triggered by faulty heart rhythms. It should not be confused with a heart attack, which is actually a blockage in one of the major blood vessels of the circulatory system. Certainly a heart attack could eventually become cardiac arrest if left untreated, but qualitatively they are entirely different events.

Whereas heart blockages and similar "plumbing problems" can be remedied by angioplasty or bypass surgery, SCA requires immediate intervention. Typically the window for successful interruption of a cardiac arrest episode will close within approximately eight to ten minutes of onset. Even with proper training, like a CPR or First Aid course that incorporates the use of an AED, SCA results in death for most out-of-hospital patients. This is certainly not for lack of trying, there are just two big problems victims currently face:

- CPR is an inefficient substitute for the natural blood delivery to the heart, and
- AEDs are only effective against two arrhythmia, v-fib and v-tach.

Ideally, technology will be made widely available so that *any* arrhythmia could be treated in an out-of-hospital environment by a layperson.

Our research has not discovered the technology described above. However, it is a step in the right direction. It is my most sincere belief that such technology can exist, and I suspect we will see it in the near future as the research progresses. In the meantime, I hope that our journey will prove useful for those looking to advance the areas of electrocardiography and AED engineering.

References

[1] ALBERTS, B. *Essential Cell Biology, 3rd Ed.* Garland Science, New York, 2010.

[2] ARMBRUSTER, D. The "almost" complete dynamics of the Fitzhugh-Nagumo equations. *World Scientific* (1997), 89 – 102.

[3] AXLER, S. *Linear Algebra Done Right*, Second ed. Springer Science + Business Media, LLC, New York, 1997.

[4] BAKER, JOHN W. Stability Properties of a Second Order Damped and Forced Nonlinear Differential Equation. *SIAM Journal of Applied Mathematics 27*, 1 (1974).

[5] BRAAKSMA, B. Critical Dynamics of the Bonhoeffer - van der Pol equation and its chaotic response to periodic stimulation. *Physica. D: Nonlinear Phenomena 68*, 2 (1993), 265 – 280.

[6] BRAUER, F., AND NOHEL, J. A. *Qualitative Theory of Ordinary Differential Equations: An Introduction*. W. A. Benjamin, Inc., New York, 1969.

[7] BRAY, W. O. Lecture 6: The Fitzhugh-Nagumo Model. Online Lecture.

[8] BROWNE, M.W. In Heartbeat, Predictability Is Worse Than Chaos. http://www.nytimes.com/1989/01/17/science/in-heartbeat-predictability-is-worse-than-chaos.html, January17 1989.

[9] BURDEN, R. L., AND FAIRES, J. D. *Numerical Analysis: Eighth Edition.* Brookes/Cole, Belmont, CA, 2005.

[10] CAIN, J. W. Taking Math to Heart: Mathematical Challenges in Cardiac Electrophysiology. *Notice of the AMS 58*, 4 (April 2011), 542 – 549.

[11] CARDIAC LIFE PRODUCTS, INC. NYSAED. http://www.nysaed.com, 2011.

[12] CHEN, J. ET AL. High-frequency periodic sources underlie ventricular fibrillation in the isolated rabbit heart. *Circulation Research: Journal of the American Heart Association*, 86 (2000), 86 – 93.

[13] FITZHUGH, R. Thresholds and Plateaus in the Hodgkin-Huxley Nerve Equations. *The Journal of General Physiology 43* (1960), 867 – 896.

[14] FITZHUGH, R. Impulses and Physiological States in Theoretical Models of Nerve Membrane. *Biophysical Journal 1* (1961), 445 – 466.

[15] HEART RHYTHM FOUNDATION. Sudden Cardiac Arrest Key Facts. http://www.heartrhythmfoundation.org/facts/scd.asp.

[16] IZHIKEVICH, E. M. *Dynamical Systems in Neuroscience: The Geometry of Excitability and Bursting*. The MIT Press, Cambridge, MA, 2010.

[17] KOSTOVA, T., RAVINDRAN, R., AND SCHONBEK, M. Fitzhugh-Nagumo Revisited: Types of Bifurcations, Periodical Forcing and Stability Regions by a Lyapunov Functional.

[18] KUZNETSOV, Y. A. *Elements of Applied Bifurcation Theory, Second Edition*, vol. 112. Springer, New York,1998.

[19] LOGAN, J. D. *Applied Partial Differential Equations.* Springer Science + Business Media, LLC, New York, 2004.

[20] LORENZ, E. N. *The Essence of Chaos.* University of Washington Press, Seattle, WA, 1993.

[21] LYNCH, S. *Dynamical Systems with Applications using Maple, 2nd Ed.* Birkhäuser, Boston, MA, 2010.

[22] MORRISON, F. *The Art of Modeling Dynamic Systems: Forecasting for Chaos, Randomness and Determinism*. Dover Publications, Inc., Mineola, NY, 2008.

[23] NAGLE, R. K., SAFF, E. B., AND SNIDER, A. D. *Fundamentals of Differential Equations and Boundary Value Problems, 5th Ed.* Pearson Education Inc., Boston, MA, 2008.

[24] POOLE, D. *Linear Algebra A Modern Introduction*, third ed. Brookes/Cole, Boston, MA, 2011.

[25] RANGARAJAN, G. Lyapunov Exponents without Rescaling and Reorthogonalization. *Physical Review Letters 80* (1998), 3747 – 3750.

[26] ROCSOREANU, C., A. GEORGESCU AND N. GIURGITEANU. *The Fitzhugh-Nagumo Model*, vol. 10. Kluwer Academic Publishers, Doredrecht, The Netherlands, 2000.

[27] SEARS, F. W. *University Physics*, 5th ed. Addison-Wesley Publishing Company, Reading, MA, 1977.

[28] SKELTON, B. Personal Interview. ZOLL Medical Corporation, Mar. 25 2010.

[29] STROGATZ, S. H. *Nonlinear Dynamics and Chaos*. Perseus Books Publishing, LLC, Cambridge, MA, 1994.

[30] TAUBES, C. H. *Modeling Differential Equations in Biology*. Prentice Hall, Inc., Upper Saddle River, NJ, 2001.

[31] THOMPSON, D. W. *On Growth and Form: The Complete Revised Edition*. Dover Publications, Inc., New York, 1992.

[32] VAN DER POL, B., AND VAN DER MARK, J. The heartbeat considered as a relaxation oscillation, and an electrical model of the heart. *The London, Edinburgh and Dublin philosophical magazine and journal of science 6* (1928), 763 – 775.

[33] WINFREE, A. T. *The Geometry of Biological Time*. Springer - Verlag New York, Inc., New York, 1980.

[34] WOLF, A. Determining Lyapunov Exponents from a Time Series. *Physica 16D* (1985), 285 – 317.